Transcriptome profiling of developing leaf and shoot apices to reveal the molecular mechanism and co-expression genes responsible for the wheat heading date

Yuxin Yang
Institute of Crop Sciences, CAAS
Xueying Zhang
Institute of Crop Sciences, CAAS
Lifen Wu
Institute of Crop Science, Chinese Academy of Agricultural Sciences
Lichao Zhang
Institue of Crop Sciences, CAAS
Guoxiang Liu
Institute of Crop sciences, CAAS
Chuan Xia
Institute of Crop Sciences, CAAS
Xu Liu
Institute of Crop Sciences, CAAS
Xiuying Kong (kongxiuying@caas.cn)
Institute of Crop Sciences, CAAS

Research article

Keywords: Wheat, Heading date, Gene expression, Transcriptional factors, Weighted gene co-expression network analysis

Posted Date: December 10th, 2020

DOI: https://doi.org/10.21203/rs.3.rs-51787/v2

Abstract

Background: Wheat is one of the most widely planted crops worldwide. The heading date is important for wheat environmental adaptability; it not only controls flowering time but also determines the yield component in terms of the grain number per spike.

Results: In this research, homozygous genotypes with early and late heading dates derived from backcrossed progeny were selected to conduct RNA-seq analysis at the double ridge stage (W2.0) and androgynous primordium differentiation stage (W3.5) of the leaf and apical meristem, respectively. In total, 18,352 differentially expressed genes (DEGs) were identified, many of which are strongly associated with the wheat heading date genes. Gene Ontology (GO) enrichment analysis revealed that carbohydrate metabolism, trehalose metabolic process, photosynthesis, and light reaction are closely related to the flowering time regulation pathway. MapMan metabolic analysis showed that the DEGs mainly functioned in light reaction, hormone signaling, lipid metabolism, secondary metabolism, and nucleotide synthesis. In addition, 1,225 DEGs were annotated to 45 transcription factor gene families, including LFY, SBP, and MADS-box transcription factors that closely related to the flowering time. Weighted gene co-expression network analysis (WGCNA) showed that 16, 336, 446, and 124 DEGs had biological connections with *Vrn1-5A*, *Vrn3-7B*, *Ppd-1D*, and *WSOC1*, respectively. Furthermore, *TraesCS2D02G181400* is a MADS-MIKC transcriptional factor that is co-expressed with *Vrn1-5A*, which indicates this gene is a potential gene related to the flowering time

Conclusions: The RNA-seq analysis enriched the transcriptome data of wheat heading date at the key flower development stages of double ridge (W2.0) and androgynous primordium differentiation (W3.5). Based on the DEGs, the co-expression networks of key flowering time genes in *Vrn1-5A*, *Vrn3-7B*, *WSOC1*, and *Ppd-1D* were established. Moreover, we discovered a potential candidate flowering time gene *TraesCS2D02G181400*. Taken together, these results serve as a foundation for further study on the regulatory mechanism of wheat heading date.

Background

Wheat (*Triticum aestivum* L.) is one of the most important and widely distributed food crops in human society. The wide global planting area of bread wheat is attributed to its high adaptability to the natural environment. Heading date or flowering time is an important adaptive trait for crop genetic breeding.

Heading date regulation networks mainly include vernalization, photoperiod, and hormones (such as gibberellin) [1, 2]. There are three important regulatory genes in the vernalization pathway: *Vernalization1* (*Vrn1-5A*, *Vrn1-5B*, *Vrn1-5D*) [3-6], *Vernalization2* (*Vrn2*) [1, 4], and *Vernalization3* (*Vrn3*) [3-6]. *Vrn1* can promote flowering and has three homologous genes in wheat: *Vrn1-5A*, *Vrn1-5B*, and *Vrn1-5D*. *Vrn-2* is the main flower suppressor gene, and it is downregulated by vernalization and short-day treatment [1, 4, 7]. *Vrn-3* is a mobile signal protein that moves from the leaf to the apical meristem and induces flowering time [1, 8]. The wheat response to the photoperiod is mainly controlled by the *photoperiod* (*Ppd*) genetic locus, and genes participating in the photoperiod pathway mainly include *Ppd-A1*, *Ppd-B1*, and *Ppd-D1* [9, 10]. Previous studies reported that *Ppd-1* plays a key role in the inflorescence morphological structure and young spike development process [11], and *Ppd-1* accelerates flowering by upregulating *Vrn3* expression under long-day conditions [12, 13]. Wheat *SOC1* (*WSOC1*) is a key regulatory gene in the gibberellin regulation pathway and affects the heading date in polyploid wheat [14]; upregulation of *WSOC1* can accelerate spike development [15].

Flower development in higher plants mainly occurs in three stages: the floral induction phase, the floral primordia phase, and the floral organ development phase. The double ridge and androgynous primordium differentiation are key stages for flower induction and floral meristem development in wheat. According to a previous study, at the double ridge stage (W1.5-W2.0), from the base of the growth cone, spikelet protuberance appears between axils of bract

primordium and determines the number of spikelets on each spike of wheat; at the differentiation stage of the androgynous primordium, the first floret primordium at the base of the spikelet begins to differentiate, and the stem begins to extend (W3.5) [16]. Thus, to explore the molecular mechanism underlying heading date, we performed RNA-seq analysis of two wheat accessions with a significant difference in heading date at W2.0 and W3.5.

In recent years, with the completion of hexaploidy bread wheat reference genomes (IWGSC, 2018), use of the bioinformatics method to discover flowering time genes and to examine molecular characterization has significantly accelerated the study of wheat flowering time. More than nine hundred flowering time genes have been identified in wheat by BLAST searches and OrthoMCL clustering methods [17]. Moreover, researchers have discovered eighty-four SNPs that are highly related to spike numbers based on GWAS [18]. Using the Bulked Segregant RNA-Seq method, a large deletion in the first intron of *Vrn-B1* causing heading date variation was identified, and some flowering time GO terms were identified [19].

However, wheat is a hexaploid species and has a complex genome, which poses a challenge for discovering flowering time genes and revealing their genetic characteristics. Here, homozygous genotypes with an early heading date (WHd) and late heading date (MHd) were selected for RNA-seq. We aimed to investigate transcriptional regulation at the two key flower development stages of double ridge and androgynous primordium differentiation, and to identify the important flowering time genes using weighted gene co-expression network construction. We anticipate that we could explore the molecular characteristics of wheat flowering time and promote the wheat improvement process through transcriptome analysis.

Results

Generation of RNA-seq data

In this study, we constructed 24 RNA-seq libraries of the 8 treatments, WHd-A2.0, MHd-A2.0, WHd-L2.0, MHd-L2.0, WHd-A3.5, MHd-A3.5, WHd-L3.5 and MHd-L3.5, and each treatment included 3 biological repeats. After high-throughput sequencing, each sample contained 40 – 59.4 million reads, the data size ranged from 6 – 8.9 Gb, the Q30 value exceeded 87%, the GC content distribution was 50 – 56%, and sequencing alignment analysis results showed that 89.35 – 97.79% of the reads could be mapped to IWGSC RefSeq v1.1 (Table S1). Principal component analysis (PCA) of the eight raw sequencing datasets indicated that the samples could be clustered into four groups according to their genotype, which showed good repeatability between samples that could be used for subsequent analysis (Fig. S1).

Identification of differentially expressed genes

To identify genes that differed significantly between the early and late heading genotypes during the development of young panicles, we analyzed the differentially expressed genes (DEGs) with strict quality control. The DEGs of L2.0, L3.5, A2.0, and A3.5 were compared between the genotypes with an early heading time (WHd) and a late heading time (MHd). Finally, we identified 18,325 unique DEGs (Fig. 1a, Table S2), which were mainly distributed at the end of the chromosome arm (Fig. S2). Specifically, there were 12,941 DEGs in the apical meristem at A2.0, 9,990 of which were upregulated and 2,951 of which were downregulated (Fig. S3a); 1,557 DEGs at A3.5, 1,406 of which were upregulated and 151 of which were downregulated (Fig. S3b), 6,390 DEGs at L2.0, 2,735 of which were upregulated and 3,655 of which were downregulated (Fig. S3c), 1,040 DEGs at L3.5, 764 of which were upregulated and 276 of which were downregulated (Fig. S3d). Flowering time genes *Vrn1-5A* [3], *Vrn3-7B* [5], *Ppd-1D* [9, 10], and *WSOC1* [14] were also found to express differentially. We also screened the common differentially expressed genes at different developmental stages in the same tissue and found that 1,084 genes were common DEGs at A2.0 and A3.5 (Fig. 1b), and 215 genes were common DEGs at L2.0 and L3.5 (Fig. 1c). We speculated that these genes may play important

roles in spikelet development at the W2.0 and W3.5 stages. Moreover, nine genes were selected from the above DEGs to assess the expression using qRT-PCR (Fig. 2a and 2b). The results showed that the expression patterns were consistent with the transcriptome analysis (Fig. 2c and 2d).

GO enrichment analysis of differentially expressed genes

To explore the regulatory pathways of DEGs, GO enrichment analyses were conducted between the early heading date and the late heading date wheat accessions. We finally identified 468 unique GO terms (Table S3, Fig. 3) that were involved in biological process (BP), molecular function (MF), and cellular component (CC) (Fig. 3a; Fig. S4; Fig. S5; Fig. S6). There were 222, 92, 208, and 127 significant GO terms in A2.0, A3.5, L2.0, and L3.5, respectively (Table S3). Interestingly, we discovered several flowering time-related GO terms, including GO:0005975 (carbohydrate metabolism) [20], GO:0005991 (trehalose metabolic process) [21], and GO:0019684 (photosynthesis, light reaction) [22]. Furthermore, we found 5 common GO terms, e.g., GO:0003700 (transcription factor activity, sequence-specific DNA binding), GO:0001071 (nucleic acid binding transcription factor activity), GO:0003824 (catalytic activity), GO:0043565 (sequence-specific DNA binding), and GO:0016491 (oxidoreductase activity), which were generally expressed in all comparative groups of DEGs (Fig. 3b).

MapMan metabolic pathway analysis of differentially expressed genes

The metabolic pathways of four comparative groups of DEGs were visualized by MapMan software (Fig. 4a; Fig. S7; Fig. S8; Fig. S9), and a total of 932 unique metabolic pathways were ultimately identified (Table S4, Fig. 4b). At A2.0, the DEGs mainly functioned in DNA.synthesis/chromatin structure (bin:28.1), signalling.receptor kinases (bin:30.2), signalling.light (bin:30.11), and hormone metabolism.jasmonate (bin:17.7). At A3.5, the DEGs function in the RNA.regulation of transcription.NAC domain transcription factor family (bin:27.3.27), PS.lightreaction.photosystem II (bin:1.1.1), hormone metabolism.ethylene.signal transduction (bin:17.5.2), protein.synthesis.initiation (bin:29.2.3). At L2.0, the metabolic pathway was mainly involved in secondary metabolism.phenylpropanoids.lignin biosynthesis (bin:16.2.1), and signalling (bin:30), RNA.regulation of transcription (bin:27.3.99). At L3.5, the DEGs were involved in DNA.synthesis/chromatin structure.histone (bin:28.1.3), transport (bin:34), metal handling.binding, chelation and storage (bin:15.2), RNA.regulation of transcription.TCP transcription factor family (bin:27.3.29). Moreover, 214 common metabolic pathways were screened, including bin:1.1.1 (light reaction), bin:11.8 (lipid metabolism), and bin:13.2.3.5 (amino acid metabolism) (Fig. 4b).

Transcription factor classification and identification

To identify the transcription factors (TFs) involved in the heading time development process, the DEGs were subjected to transcription factor analysis using iTAK software. In our study, according to the criteria of the plant transcription factor database (http://planttfdb.gao-lab.org/), a total of 1,225 transcription factors were classified into 45 transcription factor families (Table S5). A large number of DEGs were bHLH (129, 10.51%), WRKY (109, 8.88%), NAC (91, 7.41%), AP2/ERF-ERF (88, 7.17%), and MYB (64, 5.21%) transcription factors (Table S5). Among them, we also identified several transcription factor families involved in the plant flowering process, including three LFY transcription factors [23], eighteen SBP transcription factors, thirty-six MADS-MIKC transcription factors and ten MADS-M-type transcription factors (Table S5).

Gene expression level analysis showed that transcription factors were expressed at the critical period that determines flowering time. For example, we found that the three LFY transcription factor genes (*TraesCS2A02G443100*, *TraesCS2B02G464200*, *TraesCS2D02G442200*) were highly expressed in the apical meristem, especially in WHd-A3.5 and WHd-A2.0 (Fig. 5a). Most of the SBP transcription factor genes were highly expressed in WHd-A2.0 and WHd-A3.5

(Fig. 5b). In the MADS-box gene family, we discovered that the *TraesCS5A02G391700* (*Vrn1-5A*) gene always showed a high expression level in both wild and mutant wheat, *TraesCS3B02G612600* was highly expressed in leaf tissue, and two genes (*TraesCS3D02G284200*, *TraesCS3A02G284400*) were highly expressed in the apical meristem (Fig. 5c).

Construction of the flowering gene regulatory network

In our study, a total of 18,352 DEGs were used to construct the co-expression network. We calculated the average gene connectivity under different soft-thresholding powers and found that when β = 14, the co-expression network had scale-free characteristics (Fig. S10a; Fig. S10b; Fig. S10c; Fig. S10d). Finally, a total of 17 co-expression modules were obtained by the "dynamic tree cut" method. Each branch in the cluster tree represents a gene set, and different modules were distinguished by different colors (Fig. S10e). The correlation value between co-expression modules and samples was also calculated (Fig. S11). The reported flowering time genes *Vrn1-5A* (*TraesCS5A02G391700*), *Vrn3-7B* (*TraesCS7B02G013100*), *Ppd-1D* (*TraesCS2D02G079600*), and *WSOC1* (*TraesCS4D02G341700*) were selected to build a gene co-expression network, and genes connected to the reported flowering time genes were extracted from the co-expression modules. We finally detected 16, 336, 446 and 124 DEGs with biological connections to *Vrn1-5A* (Fig. 6a), *Vrn3-7B* (Fig. S12a), *Ppd-1D* (Fig. S13a), and *WSOC1* (Fig. S14a), respectively. The completed gene list related to the reported flowering time genes is summarized in Table S6.

Analysis of gene expression patterns co-expressed with *Vrn1-5A*, *Vrn3-7B*, *Ppd-1D*, and *WSOC1*

To further study the gene expression pattern of the differentially expressed genes co-expressed with the wheat heading date genes (*Vrn1-5A*, *Vrn3-7B*, *Ppd-1D*, and *WSOC1*), we found that the 16 genes that were co-expressed with *Vrn1-5A* could be divided into three patterns according to their gene expression level. First, *TraesCS2D02G181400* is a MADS-MIKC transcription factor that was highly expressed in WHd-A3.5, MHd-A3.5, MHd-L3.5, and WHd-A2.0 but expressed at low levels in WHd-L2.0, MHd-L2.0, MHd-A2.0, and WHd-L3.5 (Fig. 6b). *TraesCS2D02G181400* was upregulated between WHd-A2.0 and MHd-A2.0 and downregulated between WHd-L3.5 and MHd-L3.5 (Fig. 6c). Additionally, the other five genes (*TraesCS1D02G339300*, *TraesCS2A02G562100*, *TraesCS3A02G007200*, *TraesCS3B02G361000* and *TraesCS4D02G337000*) were expressed at low levels at all stages in both the early and late heading date accessions (Fig. 6b). In addition, the remaining ten differentially expressed genes (*TraesCS3A02G231100*, *TraesCS3B02G152300*, *TraesCS3B02G213900*, *TraesCS3B02G260400*, *TraesCS5D02G386500*, *TraesCS6A02G146500*, *TraesCS7A02G439300*, *TraesCS7A02G489000*, *TraesCS7D02G429000* and *TraesCS7D02G475300*) showed higher expression levels in WHd-L2.0, WHd-L3.5, and MHd-L2.0 but presented lower expression in WHd-A2.0, WHd-A3.5, MHd-A2.0, MHd-A3.5, and MHd-L3.5 (Fig. 6b). The genes highly related to *Vrn3-7B* were mainly expressed in the leaf tissues (Fig. S12b). Genes associated with *Ppd-1D* tended to be expressed in the leaf (Fig. S13b). Some genes that were co-expressed with *WSOC1* were preferentially expressed in leaf tissues (Fig. S14b). Furthermore, by gene function annotation, we found some vital candidate flowering time genes in the co-expression network, such as *TraesCS1A02G220300*, *TraesCS2D02G181400*, *TraesCS3A02G143100* (Fig. 2), and *TraesCS5A02G166100* (Table 1).

Discussion

Flowering time is an important agronomic trait that is regulated by many genes. The double ridge stage (W2.0) and androgynous primordium differentiation stage (W3.0) are vital during flower development. However, there are few studies on transcriptome analysis of heading date at W2.0 and W3.5 and few studies on co-expression networks construction of flowering time genes in wheat. In our study, we not only found that the known key regulated heading date genes were differentially expressed, such as *Vrn1-5A*, *Vrn3-7B*, *Ppd-1D*, and *WSOC1* [3, 9, 14] but also identified new DEGs involved in the wheat heading date process.

For example, GO:0005975 (carbohydrate metabolism) is enriched in A2.0 and L2.0, and GO:0005991 (trehalose metabolic process) is enriched in A2.0 and L3.5. A previous study reported that carbohydrate is function in the regulation of plant flowering, trehalose-6-phosphate (t6p) is suggested as an indicator to measure the carbohydrate status in plants [20, 21], and GO:0019684 (photosynthesis, light reaction) is only enriched at L3.5, which is important for photoperiod pathways [22]. The gene function annotation revealed that *TraesCS1A02G339300* and *TraesCS1B02G351600* are both trehalose-6-phosphate (t6p) (Table S2), and through MapMan metabolic pathway analysis, we discovered it was involved in the minor CHO metabolism.trehalose.TPP (bin:3.2.1). The t6p is an important endogenous signal that can influence the flowering time of *Arabidopsis thaliana* in both the shoot apical and leaves [20]; thus, we speculate that *TraesCS1A02G339300* and *TraesCS1B02G351600* can be used to reveal the molecular mechanism of t6p affecting flowering in wheat. Furthermore, gene function annotation revealed that *TraesCS3A02G400000* is a pfkB-like carbohydrate kinase family protein (Table S2), and according to MapMan analysis, we found that it participated in the major CHO metabolism.degradation.sucrose.fructokinase (bin:2.2.1.1).

Transcription factors play important roles in the regulation of plant flowering stage development. Our results showed the LFY, SBP, and MADS-box genes tended to be highly expressed in the apical meristem of wild-type wheat (WHd-A2.0, WHd-A3.5). For example, *TraesCS2A02G443100* is an LFY transcription factor; its homologous gene in rice is *Os04g0598300*, which mainly controls the heading date and determines the development of branches and tiller in the ear, overexpression of *Os04g0598300* can promote the heading date in rice [24]. In addition, one of the SBP transcription factors, *TraesCS7A02G246500,* was highly expressed at the WHd-A2.0 and WHd-A3.5 stages, and its orthologous gene in *Arabidopsis* is *ATSPL9* (*AT2G42200*). Previous research showed that *ATSPL9* can regulate flowering time by promoting the transcription of MADS-box genes, including *FUL* (FRUITFULL), *SOC1* (SUPPRESSOR OF OVEREXPRESSION OF CONSTANS 1), and *AGL42* (AGAMOUS-LIKE) [25, 26]. *TraesCS3A02G284400* is a MIKC-type MADS-box gene, and its orthologous gene in rice is *OsMADS32*. *OsMADS32* is uniquely expressed in the early stage of the inflorescence meristem, e.g., spikelet primordium, and it mainly maintains the characteristics of flower organs and regulates the development of rice flowers [27, 28]. Furthermore, we discovered that some MADS-type transcription factors were highly expressed in the leaf of both wild and mutant wheat, such as, *Vrn1-5A* (*TraesCS5A02G391700*), which indicates that this type of transcription factor can regulate flowering through different tissues, such as the leaf and apical meristem.

Moreover, many TFs, including WRKY, bZIP, bHLH, HSF, and MADS-box transcription factor genes, are also involved in the flowering time gene coexpressino network which was constructed by WGCNA (Table S6). In the *Vrn1-5A* co-expression network, we found that *TraesCS2D02G181400* is a MADS-MIKC transcription factor, which is differentially expressed in A2.0 and L3.5 (Fig. 2a and 2b), and its homologous gene in rice is *OsMADS18*, it is an AP1/FUL-like MADS-box gene that determines the formation of inflorescence meristem characteristics by interacting with PAP2 in the floral meristem [29]. We also discovered one basic helix-loop-helix (bHLH) transcription factor (*TraesCS5D02G386500*). Its homologous gene in *Arabidopsis* is *AT2G43010*, and it mainly negatively regulates the red light response mediated by phyB; thus, we speculated that red light could affect the expression of *Vrn1-5A*. In addition, *TraesCS6A02G146500* (Fig. 2) is glucose-6-phosphate 1-dehydrogenase (G6DPH) and can provide energy and other metabolites for plant growth and development, and we suggest that the expression of vernalization genes requires other genes to provide energy. In the *Vrn3-7B* gene co-expression network (Fig. S12a), we discovered four bZIP transcription factors (Table S6). Two CONSTANS-like proteins (*TraesCS5A02G166100*, *TraesCS5D02G170700*) were also discovered. The homolog of both *TraesCS5A02G166100* and *TraesCS5D02G170700* in *Arabidopsis* is *AT5G15840*, which is a zinc finger transcription factor-like protein that acts upstream of *FT* and *SOC1* and is mainly involved in flowering regulation under long-day conditions [30]. In the *Ppd-1D* co-expression network (Fig. S13a), the identified transcription factors mainly involved WRKY, bHLH, and HSF. Furthermore, we also identified one CONSTANS-

like protein gene, *TraesCS1A02G220300*. Gene function annotation showed that its homologous gene in *Arabidopsis* is *AT5G57660*, which is involved in the flowering development process [31]. From the *WSOC1* co-expression network (Fig. S14a), some WRKY and MADS-box transcription factors were also discovered. We revealed three flowering locus T genes (*TraesCS3A02G143100*, *TraesCS3B02G162000*, *TraesCS3D02G144500*), which is consistent with previous reports noting that gibberellin can activate the expression of Flowering Locus T [14]. Based on the above analysis, we suggest that the newly identified genes (*TraesCS2D02G181400*, *TraesCS5D02G386500*, *TraesCS6A02G146500*, *TraesCS5A02G166100*, *TraesCS5D02G170700*, *TraesCS1A02G220300*) associated with the reported flowering time genes (*Vrn1-5A*, *Vrn3-7B*, *Ppd-1D*, *WSOC1*) may play a key role in the wheat heading date regulatory pathway, and can be used for further research to reveal their biological functions.

Conclusions

In this study, two key flower development stages were selected to conduct RNA-seq analysis. Through DEGs analysis, many transcription factors co-expressed with the key flowering time genes (*Vrn1-5A*, *Vrn3-7B*, *Ppd-1D* and *WSOC1*) were identified by WGCNA analysis. Subsequently, a potential flowering time regulatory gene, *TraesCS2D02G181400,* was discovered from the *Vrn1-5A* network. The enriched the transcriptome data at W2.0 and W3.5 will serve as a resource for elucidating the mechanism of wheat heading date regulation.

Methods

Plant materials

m605 is a late heading mutant that was identified from the ethyl methanesulfonate mutant library of YZ4110. Previous studies conducted in our laboratory identified *m605* as a late heading mutant compared with its wild-type parent YZ4110 [32]. To reveal the molecular mechanism of the genes that regulate the heading date. The homozygous of early heading date (WHd) and late heading date phenotype (MHd) (Fig. S15) derived from the progeny of BC_3F_4 were selected to conduct the RNA-seq experiment. The purpose of using the backcrossed segregating population was to reduce the false positive problems caused by the genetic background. Seeds of each wheat accession were planted in flowerpots and grown under 16 h light/22 ℃ and 8 h dark/18 ℃ (a long-day environment) in an artificial culture room. The plants were transferred to a 4 ℃ environment for vernalization treatment for 4 weeks where they developed to the one-leaf stage and were then cultured in a greenhouse until they were sampled. A total of twenty-four wheat samples were selected, including the apex of the wild/mutant type at the W2.0/W3.5 stage (WHd-A2.0, WHd-A3.5, MHd-A2.0, MHd-A3.5) and leaves of the wild/mutant type at the W2.0/W3.5 stage (WHd-L2.0, WHd-L3.5, MHd-L2.0, MHd-L3.0). All of the plant materials used in our study were derived from the Institute of Crop Sciences, Chinese Academy of Agricultural Sciences.

RNA extraction, library construction, sequencing and quality control

The sampling period included the double ridge stage (W2.0) and androgynous primordium differentiation stage (W3.5) (Fig. S1), and the sampling position included the latest unfolding leaf and growth cone of the main stem. We used clean, liquid nitrogen-frozen forceps to quickly clamp the growth cone and place it in an RNase-free centrifuge tube (the centrifuge tube was first filled with liquid nitrogen). Newly unfolded leaves of the main stem corresponding to the growth cone were mixed at the same time; the sampling position was 2 cm away from the tip of the leaf, and a cut was made 4 cm away from the tip of the leaf to obtain a tissue sample with a length of 2 cm. All samples were rapidly frozen in liquid nitrogen and stored in a -80°C environment. The TRIzol method was used to extract the RNA from each

sample, the quality of RNA was detected by 1% agarose gel electrophoresis, and the concentration of RNA was assessed by a Nanodrop 2000 instrument. High-quality RNA samples were sent to the ONMATH company (Chengdu, China) to construct the sequencing library following Illumina's standard pipeline. The constructed sequence libraries were sequenced with the Illumina HiSeq™ 4000 platform for 150 bp paired sequencing, and raw data were saved as fastq files. To remove the adaptors and lower quality reads at the head and end, we used Trimmomatic (version 0.35) [33] to conduct quality control of sequencing data with the following parameters: java -jar trimmomatic -0.35.jar PE -threads 20 forward.fastq reverse.fastq forward_paired.fastq forward_unpaired.fastq reverse_paired.fastq reverse_unpaired.fastq ILLUMINACLIP:1.adapter.list:2:30:10 LEADING:10 TRAILING:10 SLIDINGWINDOW:1:10 MINLEN:50. FaQCs software (version 2.08) [34] was used to calculate the quality score, Q30 distribution, and GC distribution with the default parameters: FaQCs -1 R1.clean.fastq -2 R2.clean.fastq -d. –qc_only. PCA of RNA-seq data was carried out by OmicShare tools (http://www.omicshare.com/tools).

Gene expression analysis of the differentially expressed genes

RNA-seq analysis of the sequencing libraries was performed according to the method reported by Perter et al. [35]. (1) Hisat2 software (version 2.5.3a) was used to construct an index of the Chinese Spring reference genome (IWGSC RefSeq v1.1) with default parameters. (2) Raw reads were mapped to IWGSC RefSeq v1.1 by hisat2 with the parameters "hisat2 -x reference.genome.index -p 8 -X 400 –no-unal –dta -1 input.R1.clean.fastq.gz -2 input.R2.clean.fastq.gz -S input.sam", and the mapping results of reads were stored in a bam file. (3) Stringtie software (version 1.3.3b) [36] was used to carry out transcript assembly of alignments with the following parameters: stringtie -e -p 16 -B -G reference.genome.gff3 input.bam -o input.gtf. (4) The R package Ballgown [35] was used to calculate the gene expression level, and we used FPKM (fragments per kilobase of transcript per million mapped reads) to measure the gene expression value at the whole-genome level. In addition, we used HTseq-count software (version 0.11.1) [37] to count the read number of each bam file with the following command line: htseq-count –format bam –order pos –mode union –stranded no –type exon input.bam reference.genome.gtf > reference.counts.txt. The count files of reads were used to calculate the differentially expressed genes by R package egdeR [38]. The evaluation criteria of differentially expressed genes were defined as an absolute log2 (fold change) greater than 1 and a false discovery rate (FDR) less than 0.05 [39, 40]. The distribution of DEGs along three wheat subgenomes was determined by chromPlot software [41].

GO enrichment analysis of the DEGs

DEGs were submitted to the agrigo analysis toolkit [42, 43] for GO enrichment analysis. Annotation information provided by the IWGSC reference genome (IWGSC RefSeq v1.1) was used as a reference database. We used the singular enrichment analysis method through Fisher's exact and Bonferroni multiple tests to screen significant GO terms.

MapMan metabolic analysis of the DEGs

In addition, the differential expression spectrum was mapped to the metabolic regulatory pathway in detail using MapMan (version 3.5.1) [44]. Considering that MapMan software lacks the mapping file from the Chinese Spring reference genome, we first extracted the coding sequence of DEGs and then uploaded this sequence to Mercator (http://www.plabipd.de/portal/mercator-sequence-annotation) for gene annotation and to obtain the corresponding mapping file. Then, the mapping file containing the gene expression value was imported into MapMan to analyze metabolic regulation [45, 46].

Transcription factor analysis of the DEGs

To explore the transcription factor changes during wheat heading date development, we extracted the protein sequences of DEGs from IWGSC RefSeq v1.1 and used the iTAK [47] pipeline (http://bioinfo.bti.cornell.edu/tool/itak) for transcriptome factor prediction and functional classification.

Weighted gene co-expression network analysis and flowering time regulatory network construction

The R package WGCNA [48, 49] was used to construct the flowering time co-expression network and identify candidate flowering time genes. First, the “goodSamplesGenes” function was used to check the quality of the gene expression data, and the “pickSoftThreshold” function was used to determine the soft power. Second, according to the soft power value, we calculated the “adjacency matrix” and “topological overlap matrix”. Third, the initial gene expression matrix was obtained by hierarchical clustering of the dissimilarity matrix with the “hclust” function with the default parameters: minModuleSize: 30, networkType: “signed”, TOMType: “unsigned”, mergeCutHeight: 0.25. Based on the connectivity between co-expressed genes, Cytoscape software (version 3.7.2) [50] was used to visualize the flowering-related gene regulation network.

Quantitative Real-Time PCR

We used Primer Premier 5 software to design gene-specific primers based on the gene sequence. Each experiment included three biological repeats. We selected *GAPDH* (GenBank: AF251217.1) as the internal reference gene to correct the gene expression. The PCR system included a 20 μL reaction volume, which consisted of 10 μL of SYBR Mix, 2 μL of cDNA, 0.8 μL of forward and reverse primers, and 7.2 μL of ddH_2O. Then the prepared reaction volume was submitted to RT-PCR amplification in the Roche LightCycler 480 Real-Time System (Roche, Switzerland) platform. The PCR amplification steps were 95 °C for 60 seconds, followed by 40 cycles at 95 °C for 5 seconds, 60 °C for 30 seconds, and 95 °C for 15 seconds. The 2(-delta delta C(T)) method was used to conduct the relative gene expression analysis of the DEGs [51]. All of the primer sequences used in this study are shown in Table S7.

Abbreviations

DEG: Differentially expressed gene; RNA-seq: RNA sequencing; GO terms: Gene ontology terms; WGCNA: Weighted gene co-expression network analysis; EMS: Ethyl methanesulfonate; PCA: Principal component analysis; FPKM: Fragment per kilobase of transcripts effective length per million fragments mapped to all transcripts; qRT-PCR: Quantitative real-time polymerase chain reaction.

Declarations

Ethics declarations

Ethics approval and consent to participate

Not applicable.

Consent for publication

Not applicable.

Availability of data and materials

The datasets used and analyzed during the current study have been successfully stored in the SRA database of NCBI; the RNA-seq accession number is PRJNA668815 (https://www.ncbi.nlm.nih.gov/bioproject/PRJNA668815).

Competing interests

The authors declare that they have no competing interests.

Funding

This work was supported by the National Key Research and Development Program of China (2016YFD0101802), the National Natural Science Foundation of China (31371619), the National Transgenic Research Project (2016ZX08009001001-004) and Talent Program and Innovation Program of CAAS. The funders provided financial support and had no role in the study design, data analysis and interpretation, or manuscript writing.

Authors' Contributions

YY, XZ, XL and XK designed the research. YY, XZ, LW, LZ, GL and CX performed the experiments. YY and XK wrote the paper. All the authors have read and approved the manuscript.

Acknowledgements

The authors thank all who have contributed to this study.

References

1. Distelfeld A, Li C, Dubcovsky J. Regulation of flowering in temperate cereals. Current Opinion in Plant Biology. 2009;12(2):178– DOI: 10.1016/j.pbi.2008.12.010
2. Shi C, Zhao L, Zhang X, Lv G, Pan Y, Chen F. Gene regulatory network and abundant genetic variation play critical roles in heading stage of polyploidy wheat. BMC Plant Biology. 2019;19(1):6. DOI: 10.1186/s12870-018-1591-z
3. Yan L, Loukoianov A, Tranquilli G, Helguera M, Fahima T, Dubcovsky J. Positional cloning of the wheat vernalization gene *VRN1*. Proc Natl Acad Sci U S A. 2003;100(10):6263–6268. DOI: 10.1073/pnas.0937399100
4. Yan L, Loukoianov A, Blechl A, Tranquilli G, Ramakrishna W, SanMiguel P, Bennetzen JL, Echenique V, Dubcovsky J. The wheat *VRN2* gene is a flowering repressor down-regulated by vernalization. Science. 2004;303(5664):1640–1644. DOI: 10.1126/science.1094305
5. Yan L, Fu D, Li C, Tranquilli G, Bonafede M, Sanchez A, Valarik M, Yasuda S, Dubcovsky J. The wheat and barley vernalization gene *VRN3* is an orthologue of FT. Proc Natl Acad Sci U S A. 2006;103(51):19581–19586. DOI: 1073/pnas.0607142103
6. Kippes N, Zhu J, Chen A, Vanzetti L, Lukaszewski A, Nishida H, Kato K, Dvorak J, Dubcovsky J. Fine mapping and epistatic interactions of the vernalization gene *VRN-D4* in hexaploid wheat. Molecular Genetics and Genomics. 2014;289(1):47–62. DOI: 10.1007/s00438-013-0788-y
7. Dubcovsky J, Loukoianov A, Fu D, Valarik M, Sanchez A, Yan L. Effect of photoperiod on the regulation of wheat vernalization genes *VRN1* and *VRN2*. Plant Mol. Biol. 2006;60(4):469– DOI: 10.1007/s11103-005-4814-2
8. Chen A, Dubcovsky J. Wheat TILLING mutants show that the vernalization gene *VRN1* down-regulates the flowering repressor *VRN2* in leaves but is not essential for flowering. PLoS Genetics. 2012;8(12):e1003134. DOI: 10.1371/journal.pgen.1003134
9. Turner A, Beales J, Faure S. The pseudo-response regulator *Ppd-H1* provides adaptation to photoperiod in barley. Science. 2005;310(5750):1031–1034. DOI: 10.1126/science.1117619
10. Beales J, Turner A, Griffiths S, Snape JW, Laurie DA. A pseudo-response regulator is misexpressed in the photoperiod insensitive *Ppd-D1a* mutant of wheat (*Triticum aestivum*). Theor. Appl. Genet. 2007;115(5):721–733.

DOI: 10.1007/s00122-007-0603-4

11. Boden SA, Cavanagh C, Cullis BR, Ramm K, Greenwood J, Jean FE, Trevaskis B, Swain SM. *Ppd-1* is a key regulator of inflorescence architecture and paired spikelet development in wheat. Nature Plants. 2015;1(2):1–6. DOI: 10.1038/NPLANTS.2014.16
12. Shaw LM, Turner AS, Laurie DA, Baliga NS, Wang JT, Ramage D, Amin N, Schwikowski B, Ideker T. The impact of photoperiod insensitive *Ppd-1a* mutations on the photoperiod pathway across the three genomes of hexaploid wheat (*Triticum aestivum*). The Plant Journal. 2012;71(1):71–84. DOI: 10.1111/j.1365-313X.2012.04971.x
13. Nishida H, Yoshida T, Kawakami K. Structural variation in the 5' upstream region of photoperiod insensitive alleles *Ppd-A1a* and *Ppd-B1a* identified in hexaploid wheat (*Triticum aestivum*) and their effect on heading time. Mol Breeding. 2013;31(1):27–37. DOI: 10.1007/s11032-012-9765-0
14. Shitsukawa N, Ikari C, Mitsuya T. Wheat SOC1 functions independently of WAP1/VRN1, an integrator of vernalization and photoperiod flowering promotion pathways. Physiologia Plantarum. 2007;130(4):627–636. DOI: 10.1111/j.1399-3054.2007.00927.x
15. Shitsukawa N, Takagishi A, Ikari C, Takumi S, Murai K. *WFL*, a wheat *FLORICAULA/LEAFY* ortholog, is associated with spikelet formation as lateral branch of the inflorescence meristem. Genes Genet Syst. 2006;81(1):13–20. DOI: 1266/ggs.81.13
16. Waddington SR. Cartwright PM, Wall PC. A quantitative scale of spike initial and pistil development in barley and wheat. Annals of Botany. 1983;51(1):119–130. DOI:2307/2443355
17. Peng FY, Hu Z, Yang R. Genome-Wide Comparative analysis of flowering-related genes in *Arabidopsis*, wheat, and barley. International Journal of Plant Genomics. 2015;2015:1– DOI: 10.1155/2015/874361
18. Liu J, Xu Z, Fan X, Zhou Q, Cao J, Wang F, Ji G, Yang L, Feng B, Wang T. A genome-wide association study of wheat spike related traits in China. Frontiers in Plant Science. 2018;9:1584. DOI: 3389/fpls.2018.01584
19. Li Y, Xiong H, Guo H, Zhou C, Xie Y, Zhao L, Gu J, Zhao S, Ding Y, Liu L. Identification of the vernalization gene *VRN-B1* responsible for heading date variation by QTL mapping using a RIL population in wheat. BMC Plant Biology, 2020;20(1): 1–15. DOI: 10.1186/s12870-020-02539-5
20. Wahl V, Ponnu J, Schlereth A. Regulation of flowering by trehalose-6-phosphate signaling in *Arabidopsis thaliana*. Science. 2013;339(6120):704–707. DOI: 1126/science.1230406
21. Ponnu J, Wahl V, Schmid M. Trehalose-6-phosphate: connecting plant metabolism and development. Frontiers in Plant Science. 2011;2:70. DOI: 3389/fpls.2011.00070
22. Ananyev G, Gates C, Kaplan A, Dismukes GC. Photosystem II-cyclic electron flow powers exceptional photoprotection and record growth in the microalga Chlorella ohadii, Biochimica et Biophysica Acta (BBA)-Bioenergetics. 2017;1858(11):873–883. DOI: 1016/j.bbabio.2017.07.001
23. Goslin K, Zheng B, A SM, Rae L, Ryan PT, Kwaśniewska K, Thomson B, Ó'Maoiléidigh DS, Madueño F, Wellmer F, Graciet E. Transcription factor interplay between LEAFY and APETALA1/CAULIFLOWER during floral initiation. Plant Physiology. 2017;174(2):1097–1109. DOI: 10.1104/pp.17.00098
24. Nagashree KL, Ahmed MF. Electrocatalytic oxidation of methanol on Pt modified polyaniline in alkaline medium. Synthetic Metals. 2008;158(15):610–616. DOI: 1016/j.synthmet.2008.04.006
25. Wu G, Poethig RS. Temporal regulation of shoot development in *Arabidopsis thaliana* by miR156 and its target *SPL3*. 2006;133(18):3539–3547. DOI: 10.4103/0022-3859.41816
26. Yamaguchi A, Wu M, Yang L, Wu G, Poethig RS, Wagner D. The microRNA-regulated SBP-Box transcription factor SPL3 is a direct upstream activator of LEAFY, FRUITFULL, and APETALA1. Developmental Cell. 2009;17(2):268– DOI: 10.1016/j.devcel.2009.06.007

27. Wang H, Zhang L, Cai Q, Hu Y, Jin Z, Zhao X, Fan W, Huang Q, Luo Z, Chen M, et al. OsMADS32 interacts with PI-like proteins and regulates rice flower development. Journal of Integrative Plant Biology. 2015;57(5):504– DOI: 10.1111/jipb.12248
28. Sang X, Li Y, Luo Z, Ren D, Fang L, Wang N, Zhao F, Ling Y, Yang Z, Liu Y. CHIMERIC FLORAL ORGANS1, encoding a monocot-specific MADS box protein, regulates floral organ identity in rice. Plant Physiology. 2012;160(2):788– DOI: 10.2307/41694801
29. Kobayashi K, Yasuno N, Sato Y, Yamazaki R, Kimizu M, Yoshida H, Nagamura Y, Kyozuka J. Inflorescence meristem identity in rice is specified by overlapping functions of three *AP1/FUL*-like MADS box genes and *PAP2*, a *SEPALLATA* MADS box gene. The Plant Cell. 2012;24(5):1848–1859. DOI: 1105/tpc.112.097105
30. Yu Y, Qiao L, Chen J, Rong Y, Zhao Y, Cui X, Xu J, Hou X, Dong C. Arabidopsis REM16 acts as a B3 domain transcription factor to promote flowering time via directly binding to the promoters of *SOC1* and *FT*. The Plant Journal. 2020;103(4):1386–1398. DOI: 1111/tpj.14807
31. Hassidim M, Harir Y, Yakir E, Kron I, Green RM. Over-expression of *CONSTANS-LIKE 5* can induce flowering in short-day grown *Arabidopsis*. 2009;230(3):481–491. DOI: 10.1007/s00425-009-0958-7
32. Zhang X, Liu G, Zhang L, Xia C, Zhao T, Jia J, Liu X, Kong X. Fine mapping of a novel heading date gene, *TaHdm605*, in hexaploid wheat. Frontiers in Plant Science. 2018;9:1059. DOI: 3389/fpls.2018.01059
33. Bolger AM, Lohse M, Usadel B. Trimmomatic: a flexible trimmer for Illumina sequence data, Bioinformatics. 2014;30(15):2114– DOI: 10.1093/bioinformatics/btu170
34. Lo CC, Chain PSG. Rapid evaluation and quality control of next generation sequencing data with FaQCs. BMC Bioinformatics. 2014;15(1):366. DOI: 1186/s12859-014-0366-2
35. Pertea M, Kim D, Pertea GM, Leek JT, Salzberg SL. Transcript-level expression analysis of RNA-seq experiments with HISAT, StringTie and Ballgown. Nature Protocols. 2016;11(9):1650. DOI: 10.1038/nprot.2016.095
36. Pertea M, Pertea GM, Antonescu CM, Chang TC, Mendell JT, Salzberg SL. StringTie enables improved reconstruction of a transcriptome from RNA-seq reads. Nature Biotechnology. 2015;33(3):290. DOI: 10.1038/nbt.3122
37. Anders S, Pyl PT, Huber W. HTSeq - a Python framework to work with high-throughput sequencing data, Bioinformatics. 2015;31(2):166–169. DOI: 1093/bioinformatics/btu638
38. Robinson MD, McCarthy DJ, Smyth GK. edgeR: a Bioconductor package for differential expression analysis of digital gene expression data. Bioinformatics. 2010;26(1):139–140. DOI: 10.1093/bioinformatics/btp616
39. Audic S, Claverie JM. The significance of digital gene expression profiles. Genome Research. 1997;7(10):986– DOI: 10.1101/gr.7.10.986
40. Mariani TJ, Budhraja V, Mecham BH, Gu CC, Watson MA, Sadovsky Y. A variable fold change threshold determines significance for expression microarrays. The FASEB Journal. 2003;17(2):321–323. DOI: 10.1096/fj.02-0351fje
41. Oróstica KY, Verdugo RA. chromPlot: visualization of genomic data in chromosomal context, Bioinformatics. 2016;32(15):2366– DOI: 10.1093/bioinformatics/btw137
42. Du Z, Zhou X, Ling Y, Zhang Z, Su Z. agriGO: a GO analysis toolkit for the agricultural community. Nucleic Acids Research. 2010;38(Web Server issue):W64– DOI: 10.1093/nar/gkq310
43. Tian T, Liu Y, Yan H. agriGO v2. 0: a GO analysis toolkit for the agricultural community, 2017 update. Nucleic Acids Research. 2017;45(W1):W122–W129. DOI: 10.1093/nar/gkx382
44. Thimm O, Bläsing O, Gibon Y. MAPMAN: a user-driven tool to display genomics data sets onto diagrams of metabolic pathways and other biological processes. The Plant Journal. 2004;37(6):914–939. DOI: 10.1111/j.1365-313X.2004.02016.x

45. Klie S, Nikoloski Z. The choice between MapMan and Gene Ontology for automated gene function prediction in plant science, Frontiers in Genetics. 2012;3:115. DOI: 10.3389/fgene.2012.00115
46. Chandran AKN, Lee GS, Yoo YH, Yoon UH, Ahn BO, Yun DW, Kim JH, Choi HK, An G, Kim TH, et al. Functional classification of rice flanking sequence tagged genes using MapMan terms and global understanding on metabolic and regulatory pathways affected by dxr mutant having defects in light response. Rice. 2016;9(1):1–12. DOI:10.1186/s12284-016-0089-2
47. Zheng Y, Jiao C, Sun H, Rosli HG, Pombo MA, Zhang P, Banf M, Dai X, Martin GB, Giovannoni JJ. iTAK: a program for genome-wide prediction and classification of plant transcription factors, transcriptional regulators, and protein kinases, Molecular Plant. 2016;9(12):1667–1670. DOI: 10.1016/j.molp.2016.09.014
48. Zhang B, Horvath S. A general framework for weighted gene co-expression network analysis. Statistical Applications in Genetics and Molecular Biology. 2005;4(1). DOI: 10.2202/1544–1128
49. Langfelder P, Horvath S. WGCNA: an R package for weighted correlation network analysis. BMC Bioinformatics. 2008;9(1):559. DOI: 1186/1471-2105-9-559
50. Shannon P, Markiel A, Ozier O. Cytoscape: a software environment for integrated models of biomolecular interaction networks, Genome Research. 2003;13(11):2498–2504. DOI:1101/gr.1239303
51. Livak KJ, Schmittgen TD. Analysis of relative gene expression data using real-time quantitative PCR and the $2^{-\Delta\Delta C}_{T}$ Methods. 2001;25(4):402–408. DOI: 10.1006/meth.2001.1262

Tables

Table 1 Functional annotation of genes co-expressed with flowering genes.

ering gene	Candidate flowering time genes	Position in IWGSC1.1/Mb	Function annotation	Log2(FC)	*p*-value
5A	*TraesCS2D02G181400*	2D: 126.124 ~ 126.149	MADS-box transcription factor	4.72	3.90×10^{-18}
7B	*TraesCS5A02G166100*	5A: 355.071 ~ 355.072	CONSTANS-like protein	3.66	8.66×10^{-5}
	TraesCS2D02G147100	2D: 88.087 ~ 88.089	Gibberellin receptor GID1A	3.88	3.05×10^{-5}
	TraesCS5D02G170700	5D: 267.762 ~ 267.764	CONSTANS-like protein	4.16	3.56×10^{-5}
D	*TraesCS1A02G220300*	1A: 389.129 ~ 389.131	CONSTANS-like protein	-2.39	6.10×10^{-4}
	TraesCS1B02G326800	1B: 553.024 ~ 553.025	Early light-induced protein	-3.15	1.27×10^{-5}
	TraesCS1B02G326900	1B: 553.135 ~ 553.136	Early light-induced protein	-7.17	1.02×10^{-12}
	TraesCS1A02G314800	1A: 506.473 ~ 506.476	Early light-induced protein	-4.09	3.21×10^{-3}
C1	*TraesCS3A02G143100*	3A:124.172 ~ 124.176	Flowering locus T	2.74	1.69×10^{-7}
	TraesCS2B01G200800	2B: 180.040 ~ 180.060	MADS-box transcription factor	2.43	8.77×10^{-7}
	TraesCS3D01G144500	3D: 132.976 ~ 132.977	Flowering locus T	2.28	2.95×10^{-4}
	TraesCS3B02G162000	3B: 158.715 ~ 158.719	Flowering locus T	1.13	8.54×10^{-4}
	TraesCS5A02G515500	5A: 747.807 ~ 757.809	MADS-box transcription factor	1.39	8.45×10^{-4}
	TraesCS3D01G144500	3D: 132.976 ~ 132.977	Flowering locus T	2.28	2.95×10^{-4}

Figures

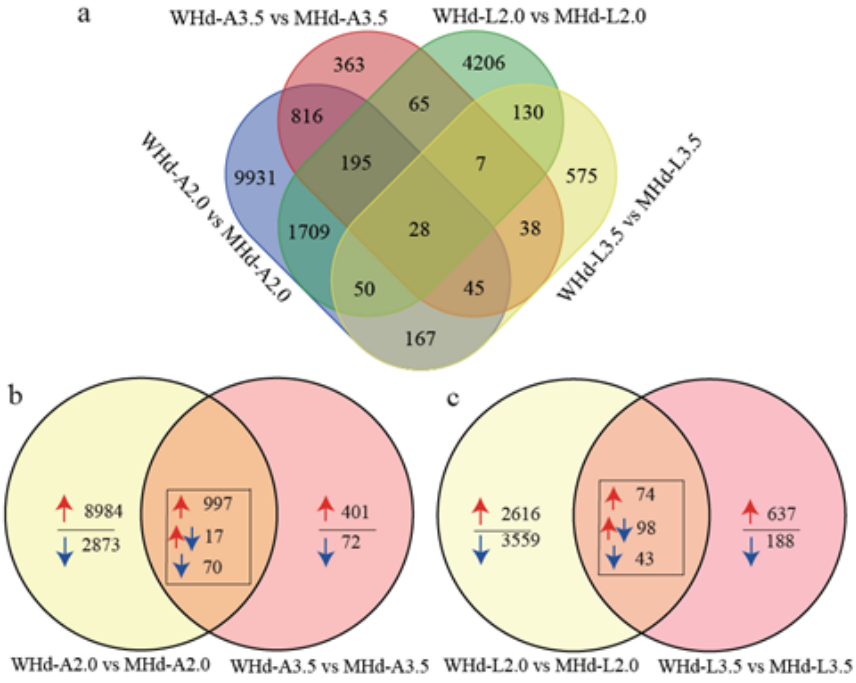

Figure 1

Venn diagram of the overall differentially expressed genes. (a) The DEGs between WHd and MHd in different tissues and development periods. (b) Common DEGs in the apex of WHd vs MHd between W2.0 and W3.5. (c) Common DEGs in leaves of WHd vs MHd between W2.0 and W3.5.

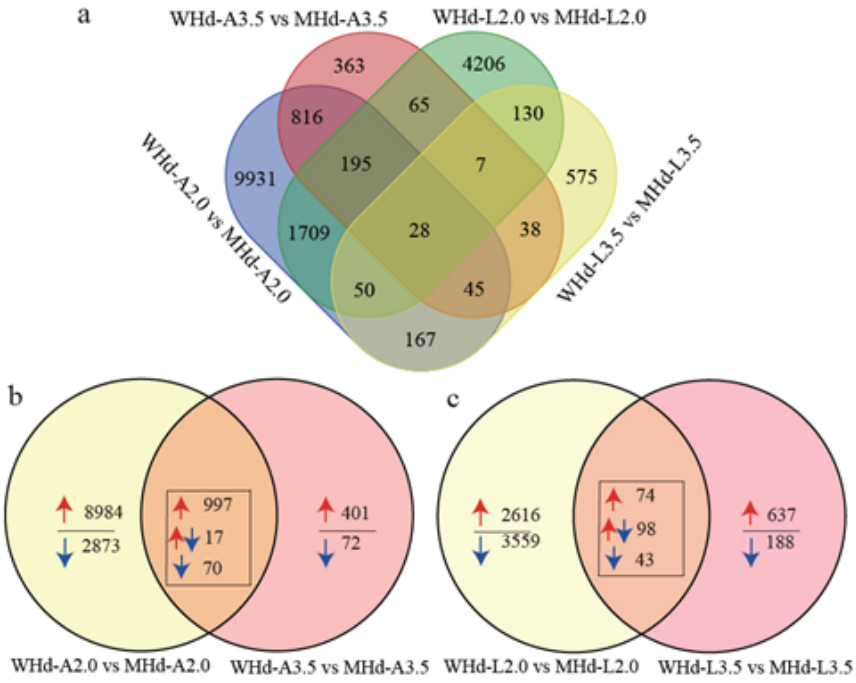

Figure 1

Venn diagram of the overall differentially expressed genes. (a) The DEGs between WHd and MHd in different tissues and development periods. (b) Common DEGs in the apex of WHd vs MHd between W2.0 and W3.5. (c) Common DEGs in leaves of WHd vs MHd between W2.0 and W3.5.

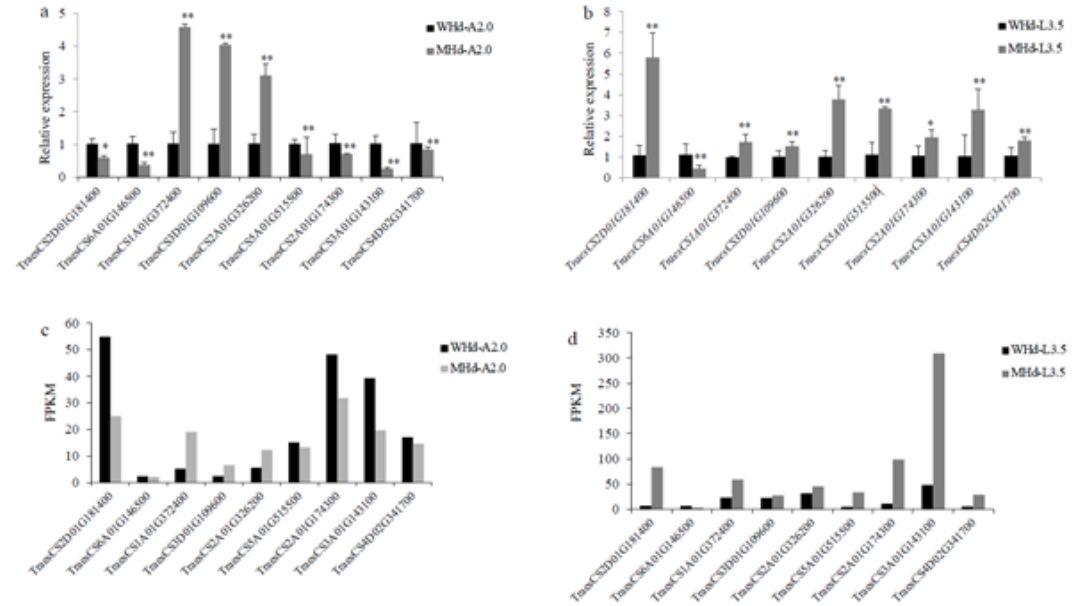

Figure 2

The gene expression level of differentially expressed genes measured using the qRT-PCR method. Each sample included three biological repeats. Three repeated biological experiments were carried out on each gene, and the error bar represents the SD of the means (n = 3). * represents the $p < 0.05$, and ** represents the $p < 0.01$. (a) The qRT-PCR results of the DEGs at A2.0. (b) The qRT-PCR results of the DEGs at L3.5. (c) The FPKM value of the DEGs at A2.0. (d) The FPKM value of the DEGs at L3.5.

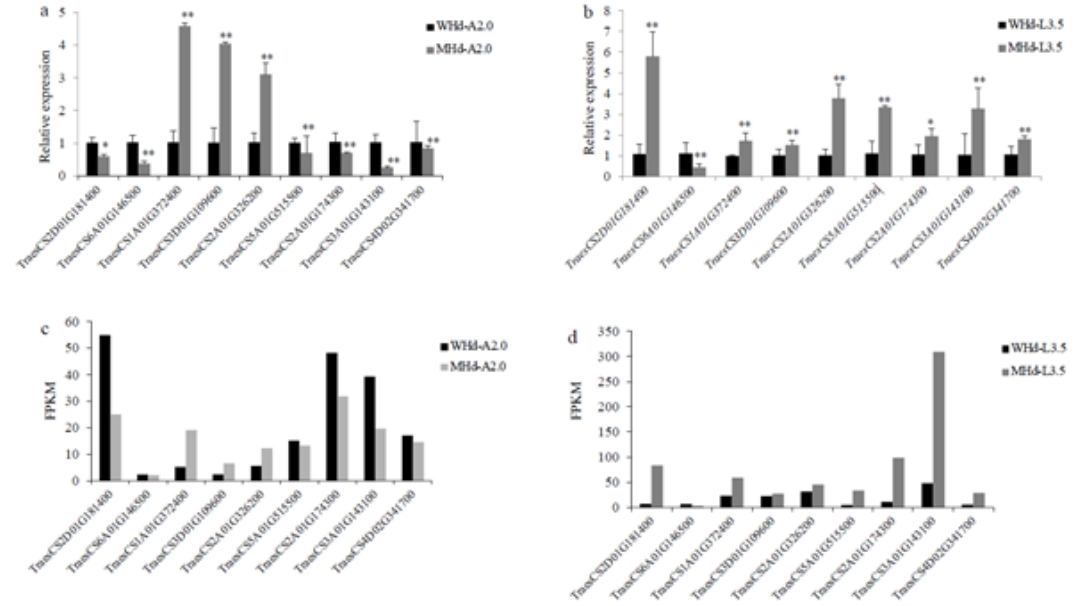

Figure 2

The gene expression level of differentially expressed genes measured using the qRT-PCR method. Each sample included three biological repeats. Three repeated biological experiments were carried out on each gene, and the error bar represents the SD of the means (n = 3). * represents the $p < 0.05$, and ** represents the $p < 0.01$. (a) The qRT-PCR results of the DEGs at A2.0. (b) The qRT-PCR results of the DEGs at L3.5. (c) The FPKM value of the DEGs at A2.0. (d) The FPKM value of the DEGs at L3.5.

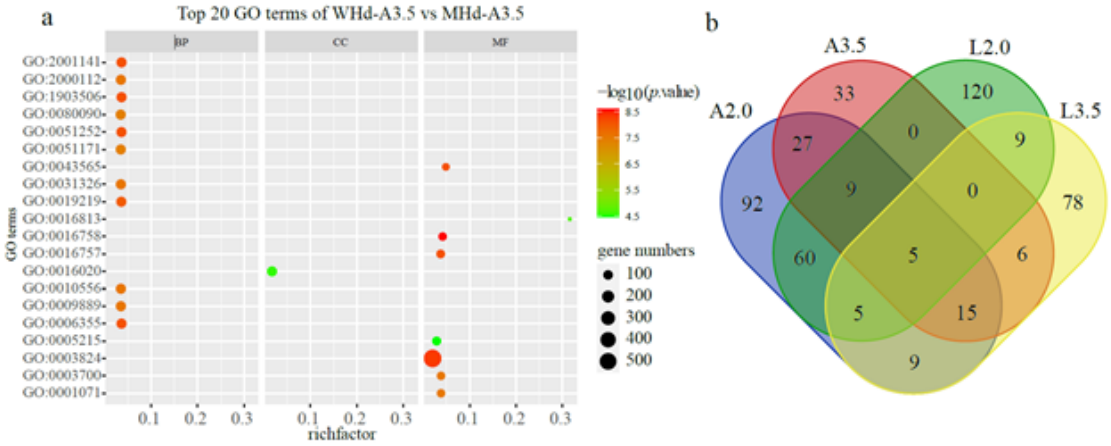

Figure 3

GO enrichment analysis of DEGs between WHd-A3.5 vs MHd-A3.5. Each row corresponds to a significant GO term, and columns represent the rich factor (gene numbers of differentially expressed genes enriched in the pathway/all gene numbers in the background gene set). The bubble size represents the gene numbers, and the color gradient represents the -log10 (p-value). (b) Venn plot showing the overlap of the number of significant GO regulatory pathways. A2.0: WHd-A2.0 vs MHd-A2.0, A3.5: WHd-A3.5 vs MHd-A3.5, L2.0: WHd-L2.0 vs MHd-L2.0, L3.5: WHd-A3.5 vs MHd-A3.5.

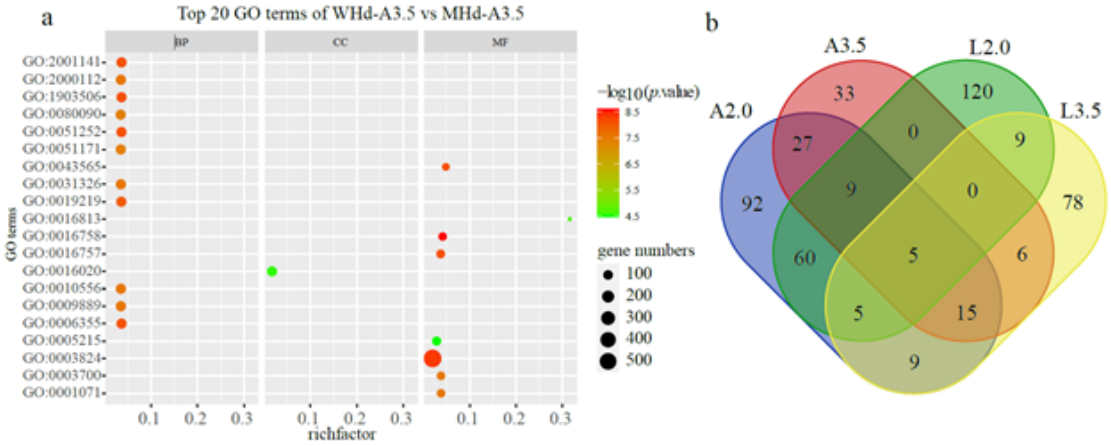

Figure 3

GO enrichment analysis of DEGs between WHd-A3.5 vs MHd-A3.5. Each row corresponds to a significant GO term, and columns represent the rich factor (gene numbers of differentially expressed genes enriched in the pathway/all gene numbers in the background gene set). The bubble size represents the gene numbers, and the color gradient represents the -log10 (p-value). (b) Venn plot showing the overlap of the number of significant GO regulatory pathways. A2.0: WHd-A2.0 vs MHd-A2.0, A3.5: WHd-A3.5 vs MHd-A3.5, L2.0: WHd-L2.0 vs MHd-L2.0, L3.5: WHd-A3.5 vs MHd-A3.5.

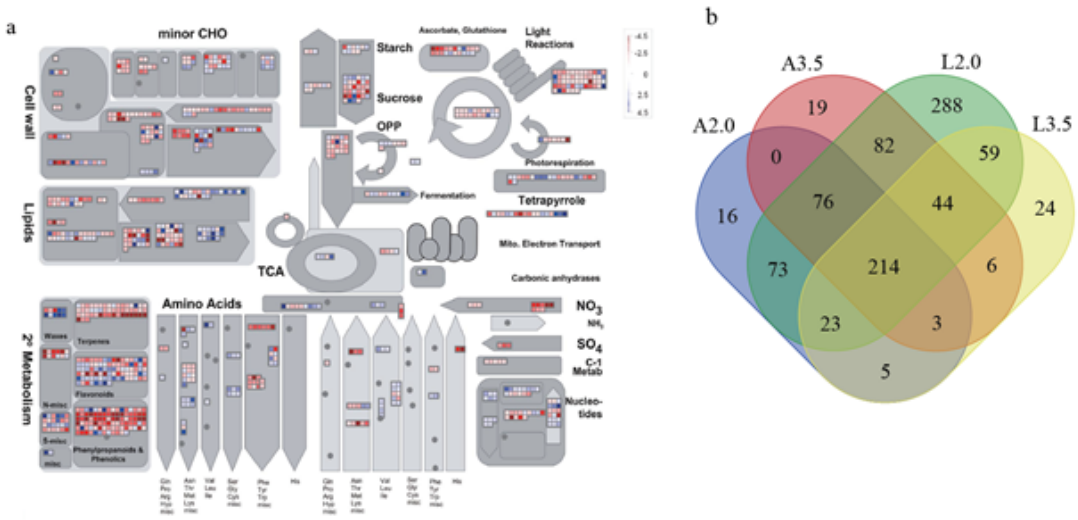

Figure 4

An overview of the metabolic pathway of differentially expressed genes between WHd-L2.0 vs MHd-L2.0. Each inset presents a differentially expressed gene. The red lattice represents the upregulated genes, and the blue lattice represents the downregulated genes. The color scale presents the fold change value of DEGs. (b) Venn diagram showing the overlap of the number of significant MapMan metabolic regulatory pathways. A2.0: WHd-A2.0 vs MHd-A2.0, A3.5: WHd-A3.5 vs MHd-A3.5, L2.0: WHd-L2.0 vs MHd-L2.0, L3.5: WHd-A3.5 vs MHd-A3.5.

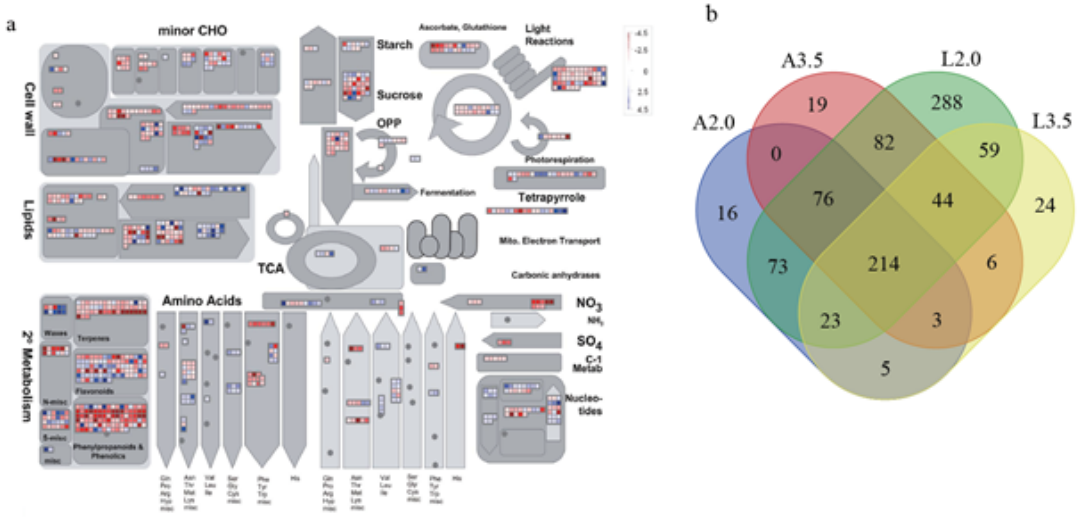

Figure 4

An overview of the metabolic pathway of differentially expressed genes between WHd-L2.0 vs MHd-L2.0. Each inset presents a differentially expressed gene. The red lattice represents the upregulated genes, and the blue lattice represents the downregulated genes. The color scale presents the fold change value of DEGs. (b) Venn diagram showing the overlap of the number of significant MapMan metabolic regulatory pathways. A2.0: WHd-A2.0 vs MHd-A2.0, A3.5: WHd-A3.5 vs MHd-A3.5, L2.0: WHd-L2.0 vs MHd-L2.0, L3.5: WHd-A3.5 vs MHd-A3.5.

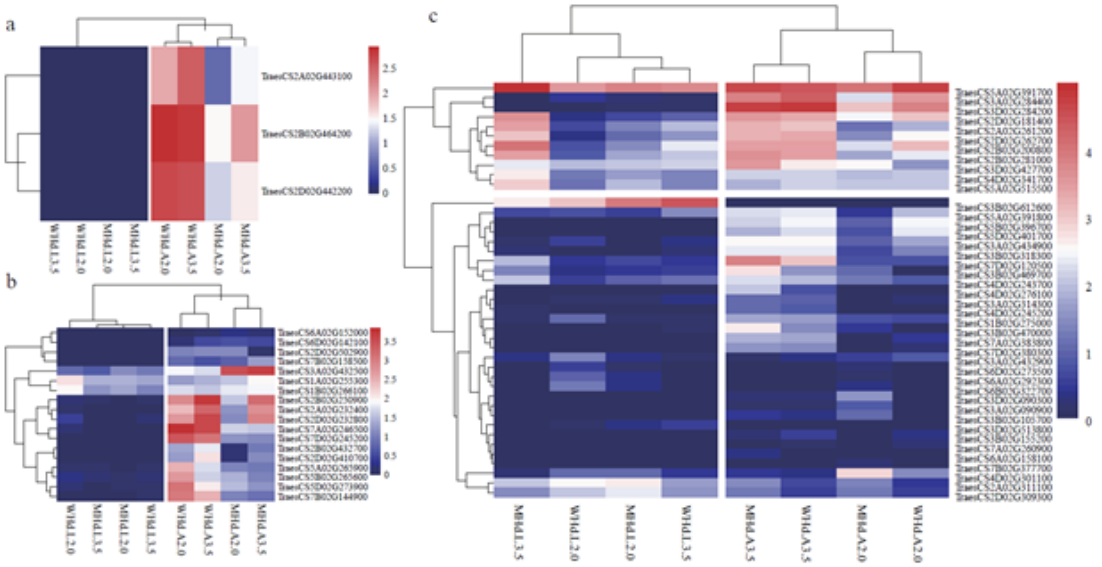

Figure 5

The gene expression level of three transcription factor gene families. (a) The LFY transcription factor gene family. (b) The SBP transcription factor gene family. (c) The MADS-box transcription factor gene family.

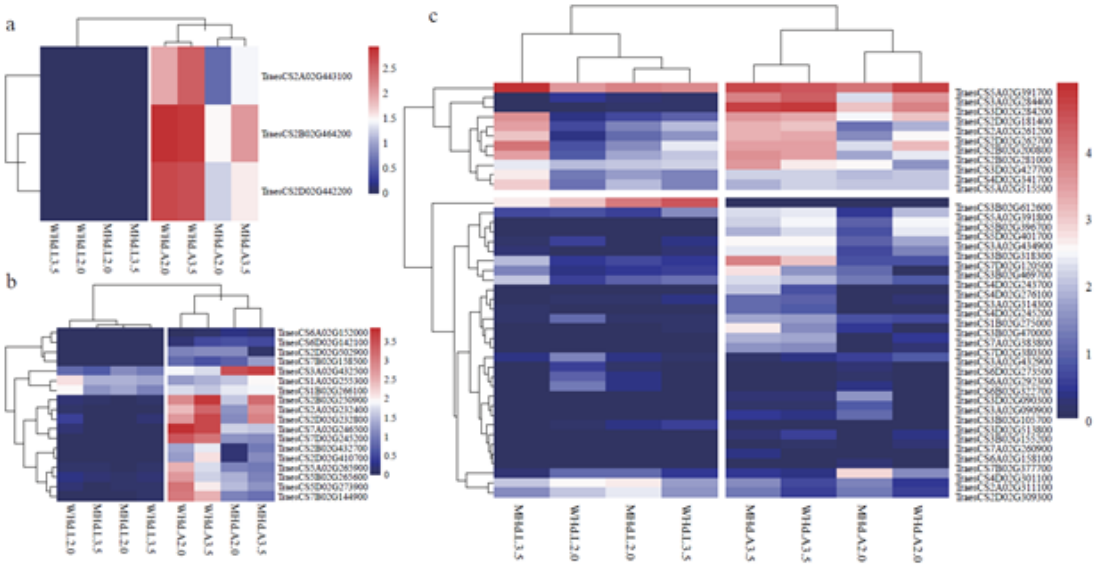

Figure 5

The gene expression level of three transcription factor gene families. (a) The LFY transcription factor gene family. (b) The SBP transcription factor gene family. (c) The MADS-box transcription factor gene family.

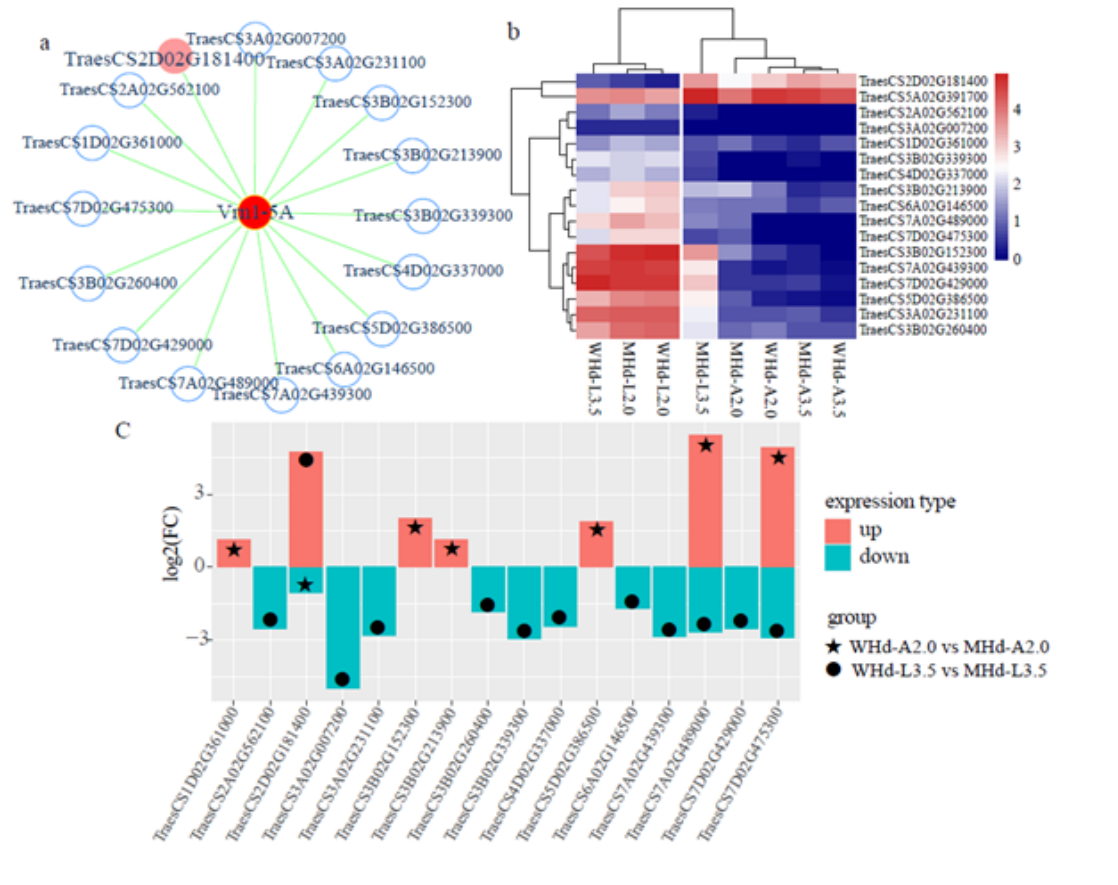

Figure 6

Construction of the flowering time regulatory network and expression level of the differential genes. The red nodes in the network indicate high-confidence genes involved in the heading date. (a) The Vrn1-5A flowering time regulatory network. (b) The expression heatmap of differentially expressed genes that were co-expressed with Vrn1-5A. (c) The expression pattern of differentially expressed genes that were co-expressed with Vrn1-5A. The red filled columns represent up-regulated genes, and the blue filled columns represent down-regulated genes.

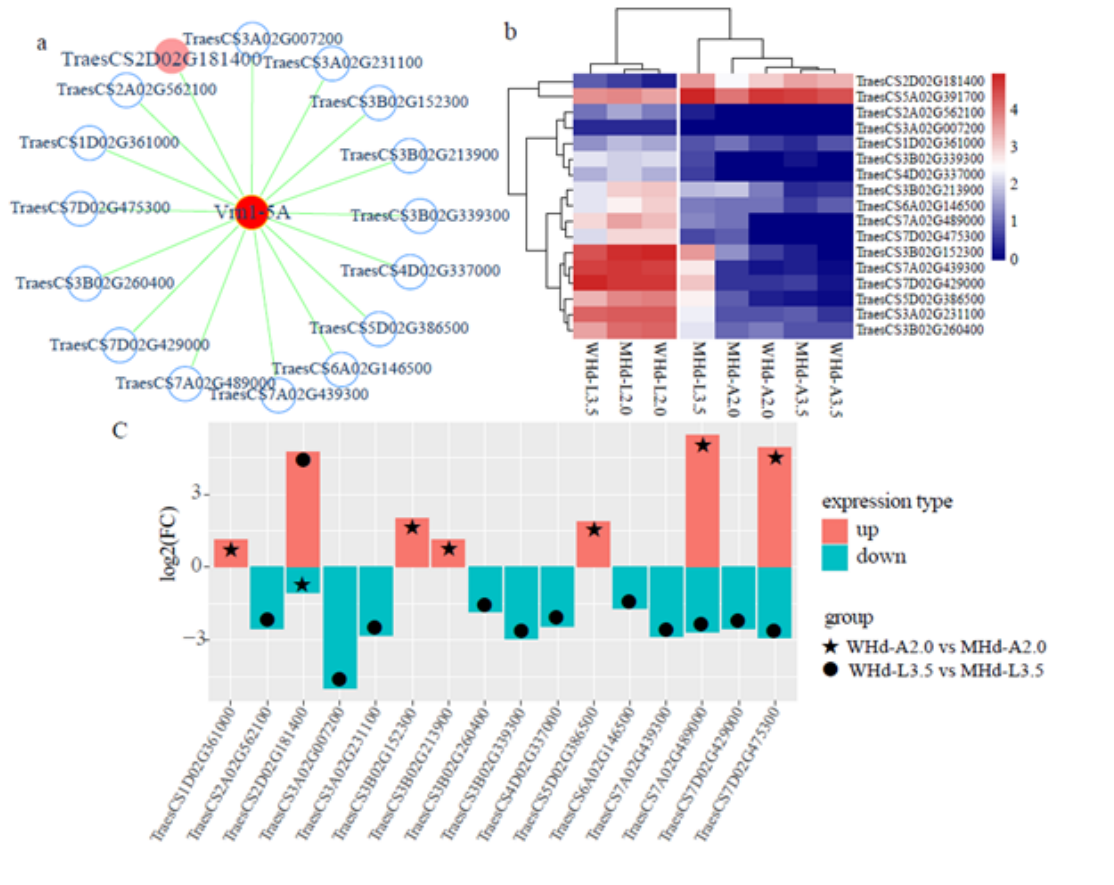

Figure 6

Construction of the flowering time regulatory network and expression level of the differential genes. The red nodes in the network indicate high-confidence genes involved in the heading date. (a) The Vrn1-5A flowering time regulatory network. (b) The expression heatmap of differentially expressed genes that were co-expressed with Vrn1-5A. (c) The expression pattern of differentially expressed genes that were co-expressed with Vrn1-5A. The red filled columns represent up-regulated genes, and the blue filled columns represent down-regulated genes.

Supplementary Files

This is a list of supplementary files associated with this preprint. Click to download.

- Additionalfile.docx
- Additionalfile.docx
- fig.s1.pdf
- fig.s1.pdf
- fig.s2.pdf
- fig.s2.pdf
- fig.s3.pdf
- fig.s3.pdf
- fig.s4.pdf
- fig.s4.pdf

- fig.s5.pdf
- fig.s5.pdf
- fig.s6.pdf
- fig.s6.pdf
- fig.s7.pdf
- fig.s7.pdf
- fig.s8.pdf
- fig.s8.pdf
- fig.s9.pdf
- fig.s9.pdf
- fig.s10.pdf
- fig.s10.pdf
- fig.s11.pdf
- fig.s11.pdf
- fig.s12.pdf
- fig.s12.pdf
- fig.s13.pdf
- fig.s13.pdf
- fig.s14.pdf
- fig.s14.pdf
- fig.s15.pdf
- fig.s15.pdf
- TableS1.xlsx
- TableS1.xlsx
- TableS2.xlsx
- TableS2.xlsx
- TableS3.xlsx
- TableS3.xlsx
- TableS4.xlsx
- TableS4.xlsx
- TableS5.xlsx
- TableS5.xlsx
- TableS6.xlsx
- TableS6.xlsx
- TableS7.xlsx
- TableS7.xlsx